The Cryosphere Discuss., https://doi.org/10.5194/tc-2019-64
Manuscript under review for journal The Cryosphere
Discussion started: 14 May 2019

The Cryosphere Discussions
Open Access
EGU

New Last Glacial Maximum Ice Thickness constraints for the Weddell Sea sector, Antarctica

Keir A. Nichols[1], Brent M. Goehring[1], Greg Balco[2], Joanne S. Johnson[3], Andrew A. Hein[4], Claire Todd[5]

[1]. Department of Earth and Environmental Sciences, Tulane University, New Orleans, 70118, LA, USA.
[2]. Berkeley Geochronology Center, 2455 Ridge Road, Berkeley, 94709, CA, USA.
[3]. British Antarctic Survey, Natural Environment Research Council, High Cross, Madingley Road, Cambridge, CB3 0ET, UK.
[4]. School of GeoSciences, University of Edinburgh, Drummund Street, Edinburgh, EH8 9XP, UK.
[5]. Department of Geosciences, Pacific Lutheran University, Tacoma, 98447, WA, USA.

Correspondence to: Keir Nichols (knichol3@tulane.edu)

Abstract. This paper describes new Last Glacial Maximum (LGM) ice thickness constraints for three locations spanning the Weddell Sea Embayment (WSE) of Antarctica. Samples collected from the Shackleton Range, Pensacola Mountains, and the Lassiter Coast constrain the LGM thickness of the Slessor Glacier, Foundation Ice Stream, and grounded ice proximal to the modern Ronne Ice Shelf edge on the Antarctic Peninsula, respectively. Previous attempts to reconstruct LGM-to-present ice thickness changes around the WSE used measurements of long-lived cosmogenic nuclides, primarily ^{10}Be. An absence of post-LGM apparent exposure ages at many sites led to LGM thickness reconstructions that were spatially highly variable, and inconsistent with flowline modeling. Estimates for the contribution of the ice sheet occupying the WSE at the LGM to global sea level since deglaciation vary by an order of magnitude, from 1.4 to 14.1 m of sea level equivalent. Here we use a cosmogenic nuclide, in situ produced ^{14}C, to evaluate the possibility that sites with no post-LGM exposure ages are biased by cosmogenic nuclide inheritance due to surface preservation by cold-based ice and nondeposition of LGM-aged drift. Our measurements show that the Slessor Glacier was between 310 and 650 m thicker than present at the LGM. The Foundation Ice Stream was at least 800 m thicker, and ice on the Lassiter Coast was at least 385 m thicker than present at the LGM. With evidence for LGM thickening at all of our study sites, our in situ ^{14}C measurements indicate that the long-lived nuclide measurements of previous studies were influenced by cosmogenic nuclide inheritance. Our LGM thickness constraints point toward a modest contribution from the Weddell Sea Embayment to global sea-level since deglaciation, with an estimated range of 2.2 to 5.8 m.

1. Introduction

This paper describes new in situ produced ^{14}C derived Last Glacial Maximum (LGM) ice thickness constraints from three locations within the Weddell Sea Embayment (WSE) of Antarctica (Fig. 1). The WSE drains approximately one fifth of the total area of the Antarctic Ice Sheet (AIS) (Joughin et al., 2006) and is thus an important contributor to LGM-to-present and, potentially, future sea-level change. Previous attempts to reconstruct LGM-to-present ice thickness changes around the WSE used measurements of long-lived cosmogenic nuclides, primarily ^{10}Be. An absence of post-LGM apparent exposure ages at many sites led to LGM thickness reconstructions that were spatially highly variable, and inconsistent with flowline modeling. Consequently, estimates based on ice models constrained by field evidence (Le Brocq et al., 2011) and by relative sea-level records and earth viscosity models (Bassett et al., 2007) for the contribution of the sector to global sea-level since deglaciation began vary by an order of magnitude, from 1.4 to 14.1 m, respectively. The lack of geological evidence for LGM thickening is also manifest in a misfit between present day geodetic uplift rate measurements in southern Palmer Land and predicted uplift rates from a glacial isostatic adjustment (GIA) model (Wolstencroft et al., 2015). Constraining the previous vertical extent of ice provides inputs to numerical models investigating both the response of the ice sheet to past and potential future changes in climate and sea-level (e.g. Briggs et al., 2014; Pollard et al., 2016; 2017;

Whitehouse et al., 2017), as well as the response of the solid earth to past ice load changes to quantify present day ice-mass loss (e.g. Wolstencroft et al., 2015). Furthermore, quantifying the LGM dimensions of the WSE sector of the AIS is required to further constrain the offset between estimates for post-LGM sea-level rise and estimates of the total amount of ice melted since the LGM. The former is sourced from sea-level index points, and the latter is sourced from our knowledge of the dimensions of ice masses at the LGM (Simms et al., 2019). Currently, the "missing ice" accounts for between 15.6 ± 9.6 m and 18.1 ± 9.6 m of global sea-level rise since the LGM (Simms et al., 2019).

Although the use of cosmogenic nuclide geochronology to study the AIS is clearly proven (e.g. Stone et al., 2003; Ackert et al., 2007), applications in the WSE are challenging. Many studies, despite making multiple cosmogenic nuclide measurements from relatively large numbers of samples, observed no or few post-LGM exposure ages (Hein et al., 2011, 2014; Balco et al., 2016; Bentley et al., 2017). With no evidence for LGM ice cover, it was not clear whether sites were covered by ice at the LGM, or whether sites were covered but the ice left no fresh deposits on top of those yielding pre-LGM ages. It is therefore currently unknown whether ice was thicker than present during the LGM at the Schmidt Hills in the Pensacola Mountains, and in the Shackleton Range (Figs. 1 and 2). Results from the Schmidt Hills (Fig. 1) indicating no LGM thickening of the Foundation Ice Stream (FIS) are particularly problematic, as thickening of 500 m from the Williams Hills, 50 km upstream of the Schmidt Hills, produces a LGM surface slope that exceeds glaciological models and present-day ice surfaces (Huybers, 2014; Balco et al., 2016). Cold-based ice and an associated lack of subglacial erosion is the likely cause of the complex ^{10}Be data sets, evidenced by numerous studies in the WSE that report ^{10}Be and ^{26}Al ratios significantly below those predicted for continuous exposure which is indicative of significant periods of burial (e.g. Bentley et al., 2006; Sugden et al., 2017). Cold-based ice preserves surfaces (Sugden et al., 2005), allowing nuclide concentrations to persist within surfaces from previous periods of exposure to the present, a phenomenon known as inheritance. Long-lived nuclides are particularly susceptible to inheritance due to their long half-lives which, without erosion beneath cold-based ice, require long periods of burial to reduce concentrations. When covered by cold-based ice during glaciations, concentrations of long-lived nuclides record exposure during multiple separate ice free periods rather than just the most recent one. Inheritance thus hinders interpretations of cosmogenic nuclide measurements.

We resolve conflicting LGM thickening estimates based on ^{10}Be measurements by using a cosmogenic nuclide largely insensitive to inheritance; in situ-produced ^{14}C. We present the in situ ^{14}C analysis of transects of erratic and bedrock samples from the Shackleton Range, Lassiter Coast and Pensacola Mountains (Fig. 1). Our results constrain LGM thickening of the Slessor Glacier to between 310 and 650 m. We show that ice was at least 385 m thicker than present during the LGM at the Lassiter Coast, proximal to the modern Ronne Ice Shelf edge. Our data also constrain LGM thickening of the FIS to at least 800 m at the Schmidt Hills. Our thickness estimates are comparable to those of Hein et al. (2016) in the Ellsworth Mountains, as well as those of Balco et al. (2016) and Bentley et al. (2017) in the Williams and Thomas Hills. Although our results show that locations around the WSE were buried by hundreds of metres of ice, this is less than called for by some reconstructions, and our inferred LGM configuration indicates a relatively modest contribution to sea-level since the LGM, with an estimate of between 2.2 to 5.8 m of sea-level equivalent.

1.1 The Last Glacial Maximum in the Weddell Sea Embayment

Although it is clear that grounded ice in the WSE has been thicker in the past (Bentley and Anderson, 1998), there is little evidence as to the thickness and grounding line position of the ice sheet at the LGM, with contrasting evidence from marine sources, and those inferred from terrestrial studies (Hillenbrand et al., 2014). Terrestrial evidence for the extent of ice in the WSE during the LGM takes the form of numerous cosmogenic nuclide studies. Bentley et al. (2006) measured the ^{10}Be and ^{26}Al content of erratics on the southern Antarctic Peninsula. Studies report cosmogenic nuclide concentrations from the Meyer Hills, Patriot Hills, Marble Hills, and the Flower Hills, all in the Ellsworth Mountains (Bentley et al., 2010; Fogwill et al, 2014; Hein et al., 2016; Sugden et al; 2017), the Pensacola Mountains (Hodgson et al, 2012; Balco et al, 2016; Bentley et al, 2017), and the Shackleton Range (Fogwill et al., 2004; Hein et al, 2011; 2014). Figure 2 summarises the ice thickness estimates from these studies. The majority of estimates are sourced from ^{10}Be measurements, with some accompanying ^{26}Al measurements. Two exceptions are Fogwill et al. (2014) and Balco et al. (2016), whom combined some in situ ^{14}C measurements with ^{10}Be measurements to constrain the thickness of the Rutford and Institute ice streams and the Foundation Ice Stream, respectively. The highest elevation post-LGM exposure ages at each site delineate the minimum

vertical extent of ice at the LGM. Ice thickness estimates vary spatially around the embayment, ranging from zero to hundreds of metres of LGM thickening.

Marine geological and geophysical evidence in the southern Weddell Sea indicates a significantly expanded WSE LGM configuration, with subglacial till, subglacial bedforms and a grounding zone wedge found towards the offshore shelf edge (Hillenbrand et al., 2012; 2014; Larter et al., 2012; Arndt et al., 2017). As a result, there is currently a disconnect between marine evidence for a greatly expanded WSE sector and terrestrial evidence indicating little to no vertical change at the LGM in some areas. Hillenbrand et al. (2014) propose two potential LGM configurations of the WSE sector of the AIS. The first scenario, based on terrestrial evidence for vertical LGM ice thicknesses, involves a complex configuration with the grounding line of the ice sheet situated towards the offshore shelf edge and a largely ice-free Filchner Trough and western margin of the WSE. The second scenario, based on marine evidence, places the grounding line of the ice sheet at the offshore shelf edge across the width of the WSE. Flowline modelling of the response of the FIS, which occupied the Filchner Trough at the LGM, to the onset of glacial conditions shows that there are two plausible LGM grounding line positions for the ice stream: one situated at the offshore shelf edge, and another at the northern margin of Berkner Island (Whitehouse et al., 2017).

1.2 In situ ^{14}C exposure dating

Cosmogenic nuclides ^{10}Be and ^{26}Al have half-lives that are much longer than glacial-interglacial cycles, so ^{10}Be and ^{26}Al concentrations produced in previous interglacials persist to the present if covered by non-erosive, cold-based ice. The short half-life of in situ ^{14}C (5730 yr) means that only short periods of burial are required to reduce concentrations from previous periods of exposure, making in situ ^{14}C less sensitive to inheritance than longer lived nuclides. Furthermore, surfaces not covered by ice during the LGM reach an equilibrium between production and decay of in situ ^{14}C ("saturation") after approximately 30 to 35 kyr. A sample measured today that has reached saturation thus requires continuous exposure from before the LGM, whilst a sample that yields a concentration below saturation requires ice cover during the last ca. 35 kyr. Surfaces yielding saturation concentrations therefore provide an upper limit on LGM thickening. Figure 3 shows a hypothetical ice surface elevation change history at a nunatak partially buried by cold-based ice during the LGM, with associated in situ ^{14}C measurements from samples collected along an elevation transect on the surface of the nunatak. There is a transition from undersaturated to saturated samples, a discontinuity in the ^{14}C concentrations which constrains the LGM ice thickness. The "true exposure" data points represent in situ ^{14}C concentrations with resulting exposure ages matching the post-LGM ice-surface lowering history. The "apparent exposure" data points were saturated at the onset of ice cover and include in situ ^{14}C that persists to the present due to an insufficient amount of time passing for it to decay away. For the five undersaturated samples, which were buried by ice for differing durations, a range of ~2 to ~4 % of the ^{14}C accumulated prior to burial will persist to the present. In terms of the effect on resulting exposure ages, the sample exposed at 10 ka yields an apparent exposure age of 11.41 ka (~13 % increase), and the sample exposed at 2 ka yields an apparent exposure age of 2.17 ka (~8 % increase). Without knowing the burial duration of the samples or whether or not the samples were indeed saturated upon burial by LGM ice, we don't know the exact quantity of in situ ^{14}C inherited in the samples. The in situ ^{14}C exposure ages are therefore maximum deglaciation ages. In the same hypothetical scenario with the same samples, ca. 98 % and 97 % of the ^{10}Be and ^{26}Al accumulated prior to burial will persist to the present, respectively.

We report in situ ^{14}C concentrations measured from both erratic and bedrock samples, with primarily erratic samples from the Shackleton Range and the Pensacola Mountains, and solely bedrock from the Lassiter Coast. We assume both materials provide the same information regarding the timing of ice retreat and constraining LGM ice thicknesses. For example, we assume that both erratics and bedrock samples saturated with in situ ^{14}C indicate that their respective sampling locations were ice free for the last 30 to 35 kyr. With the exception of two samples, all of our erratic samples have previously been measured for their ^{10}Be content (Hein et al., 2011; 2014, Balco et al., 2016), with the vast majority yielding ages far in excess of the LGM. It is highly likely that these erratic samples have been repeatedly covered and exposed by cold-based ice. Having been covered and uncovered in situ, the erratic samples can thus effectively be considered bedrock. There are, however, potential situations where our assumption is not met and resulting ^{14}C concentrations misrepresent the age of deglaciation, creating scatter in the measured in situ ^{14}C data. Erratic samples may, for example, be sourced from mass movement onto glacier surfaces, producing spuriously high ^{14}C concentrations (See Balco et al., accepted). Spuriously high, in excess of

saturation, in situ ^{14}C concentrations sourced from bedrock samples, however, can only result from analytical errors and thus provides an important test for the premise of the technique. Additionally, erratic cobbles may have undergone downslope movement post-deposition and may have flipped over which could produce in situ ^{14}C concentrations with resulting exposure ages lower than the true age of deglaciation. Snow shielding of sample locations is another mechanism leading to exposure ages which underestimate the age of deglaciation and can influence both bedrock and erratic samples. Whilst not without challenges, our in situ ^{14}C measurements provide an opportunity to unambiguously show whether sites around the WSE were covered by ice at the LGM.

1.3 Sample Sites

The purpose of this study is to resolve ambiguities in LGM ice thicknesses inferred from measurements of long-lived cosmogenic nuclides by measuring in-situ-produced ^{14}C at sites throughout the WSE, described in detail below, where ^{10}Be and ^{26}Al data provide no evidence, or conflicting evidence, for LGM ice cover.

1.3.1 Shackleton Range

The Shackleton Range is located in Coats Land in the northeast WSE, adjacent to the Slessor Glacier (Figs. 1 and 4a). The Slessor Glacier drains ice from the East Antarctic Ice Sheet (EAIS) into the Filchner Ice Shelf. Mt. Skidmore is located approximately 25 km upstream of the modern Slessor Glacier grounding zone, with the Köppen and Stratton glaciers respectively joining the Slessor Glacier to the north and south of Mt. Skidmore (Fig. 4a). Proximal to sampling locations are Ice Tongue A and Ice Tongue B of the Stratton Glacier, and the Snow Drift Glacier (Fig. S1). We assume that samples collected from Mt. Skidmore record changes in the thickness of the Slessor Glacier. However, it is possible that samples collected proximal to the smaller ice masses may have been buried by them, rather than by the Slessor Glacier, potentially complicating the interpretation of results. The modern Slessor Glacier surface is situated at ~200 m asl proximal to Mt. Skidmore, with exposed surfaces of Mt. Skidmore located up to over ~820 m asl. Mt. Provender is located adjacent to the Slessor Glacier grounding zone and is bounded by the Stratton and Blaiklock glaciers to the north and south, respectively. Exposed rock of Mt. Provender rises from the modern ice surface up to over ~900 m asl. We analysed 11 samples from the Shackleton Range (Table S1), with two from Mt. Provender and nine from Mt. Skidmore (Fig. 4a). At Mt. Provender we analysed one erratic cobble from near the modern ice surface and one bedrock sample from ~650 m above it (Fig. S2). Samples from Mt. Skidmore include one bedrock sample and eight cobbles that form an elevation transect from near the modern ice surface to ~300 m above it (Fig. S1). The two highest elevation samples collected from Mt. Skidmore are proximal to the main trunk of the Stratton Glacier more so than the Slessor Glacier, and were collected from ca. 115 and 130 m above the modern Stratton Glacier surface. The two highest elevation samples on Mt. Skidmore therefore may represent a Stratton Glacier ice surface lowering more so than the Slessor Glacier, and thus are presented as a separate sample group to those from collected proximal to the Slessor Glacier.

1.3.2 Lassiter Coast

The Lassiter Coast is located on the east coast of southern Palmer Land, adjacent to the present position of the Ronne Ice Shelf edge (Fig. 1). The modern ice surface is situated at 490 m asl. Johnson et al., (2019 in review) collected samples from several sites in this area (Fig. 4) and carried out ^{10}Be measurements; we subsequently carried out ^{14}C measurements on these samples as part of the present study, and the ^{14}C results are reported both here and in Johnson et al. (2019 in review). Here we discuss results for a total of eight bedrock samples from Mt. Lampert and the Bowman Peninsula collected from 20 to 385 m above the modern ice surface (Figs. 4 and S3); see Table S1 for sample data and Johnson et al. (in review) for ^{10}Be measurements. The adjacent Johnston Glacier drains ice from central Palmer Land into the WSE. We interpret the samples together as effectively a single elevation transect that records changes in the thickness of grounded ice in the WSE immediately east of these sites after the LGM.

1.3.3 Pensacola Mountains

The Schmidt Hills are a series of nunataks adjacent to the FIS in the southeast WSE (Figs. 1 and 4c) downstream and proximal to the modern grounding zone. The FIS is a major ice stream that drains ice from both the EAIS and West

Antarctic Ice Sheet (WAIS) into the WSE. The surface of the FIS adjacent to the Schmidt Hills is situated ca. 200 m asl., with exposed surfaces of the Schmidt Hills reaching up to 1100 m asl. The Thomas Hills are another series of nunataks adjacent to the FIS, located ~130 km upstream of the Schmidt Hills (Fig. 4d). The main trunk of the FIS adjacent to the Thomas Hills is near 550 m asl, with the Thomas Hills rising up to 1050 m asl. The local ice margin of the FIS at the Thomas Hills is situated ~75 m below the centre of the FIS. We analysed 17 samples from the Pensacola Mountains (Table S1); 15 from the Schmidt Hills and two from the Thomas Hills. We made a further seven repeat measurements from four Schmidt Hills samples. Samples from the Schmidt Hills were collected from Mount Coulter and No Name Spur (Figs. 4c and S4) from close to the modern ice surface to approximately 800 m above it. We also analysed two samples from the Thomas Hills which were collected from Mount Warnke ca. 320 m above the FIS ice margin (Figs. 4d and S5). The highest elevation sample from the Schmidt Hills, collected from ca. 1035 m asl, is the only bedrock sample analysed from the Pensacola Mountains, with the rest being erratic cobbles.

2. Methods

We analysed between 0.5 and 10 g of quartz from each sample for in situ ^{14}C analysis. The methodology used for the isolation of quartz varies for samples from different sample sites because quartz was previously isolated for prior cosmogenic nuclide studies (see Hein et al., 2011; Balco et al., 2016). For samples processed at the Tulane University Cosmogenic Nuclide Laboratory (primarily those from the Lassiter Coast), quartz was isolated through crushing, sieving, magnetic separation and froth flotation (modified from Herber, 1969) of sample material. Samples were then etched for at least two periods of 24 hours on both a shaker table in 5 % HF/HNO_3 and then in an ultrasonic bath in 1 % HF/HNO_3. This leaching procedure removes the organic compound laurylamine used in the froth flotation procedure (Nichols et al., in preparation) that could otherwise potentially contaminate our samples with modern carbon.

Carbon was extracted using the Tulane University Carbon Extraction and Graphitization System (TU-CEGS), following the method of Goehring et al. (2019). Quartz is step-heated in a lithium metaborate ($LiBO_2$) flux and a high-purity O_2 atmosphere, first at 500 °C for 30 minutes, then at 1100 °C for three hours. Released carbon species are oxidised to form CO_2 via secondary hot-quartz-bed oxidation, followed by cryogenic collection and purification. Sample yields are measured manometrically, and samples are diluted with ^{14}C-free CO_2. A small aliquot of CO_2 is collected for $\delta^{13}C$ analysis, and the remaining CO_2 is graphitised using H_2 reduction over an Fe catalyst. We measured $^{14}C/^{13}C$ isotope ratios at either Lawrence Livermore National Laboratory Center for Accelerator Mass Spectrometry (LLNL-CAMS) or Woods Hole National Ocean Sciences Accelerator Mass Spectrometry (NOSAMS) (Table S2). Stable carbon isotope ratios were measured at the UC-Davis Stable Isotope Facility.

Apparent exposure ages were calculated using v. 3 of the online calculators formerly known as the CRONUS-Earth online calculators (Balco et al., 2008). The online calculators use the production rate scaling method for neutrons, protons and muons of Lifton et al. (2014) (also known as LSDn). We use repeat measurements of the in situ ^{14}C concentration of the CRONUS-A interlaboratory comparison standard (Jull et al., 2015; Goehring et al., 2019) to calibrate the ^{14}C production rate. We assume CRONUS-A is saturated with respect to in situ ^{14}C, given that the sampling location was not covered by ice during the LGM. Repeat measurements of both CRONUS-A and other samples using the TU-CEGS show that the reproducibility of in situ ^{14}C measurements is approximately 6 %. We therefore use a 6 % uncertainty for our measured in situ ^{14}C concentrations when calculating exposure ages, as this exceeds the reported analytical uncertainty for all of our in situ ^{14}C measurements. Ages are included in Table S2 for completeness but are primarily discussed in the text as either finite or infinite ages. Infinite ages are those for which the measured concentration is above the uncertainty of the saturation concentration for the elevation of a given sample.

3.0 Results

The vast majority of the ^{10}Be ages reported by Hein et al. (2011; 2014) in the Shackleton Range exceed 100 ka, whilst we find finite ^{14}C ages at both Mt. Skidmore and Mt. Provender (Fig. 5). At Mt. Skidmore, finite ages are evident

across the entire Mt. Skidmore transect, including those sampled proximal to the Stratton Glacier (Fig. 5). Samples were collected from multiple ridges of Mt. Skidmore and thus would not necessarily be expected to form a single age-elevation line. The uppermost sample proximal to the Slessor Glacier, collected ~310 m above the modern ice surface, provides a lower limit for LGM ice thickening. The two samples proximal to the Stratton Glacier constrain LGM thickening to at least 130 m. At Mt. Provender, one sample collected proximal to the local Slessor Glacier margin yields a finite age. A second sample from ~890 m asl (~655 m above the modern ice surface) yields an infinite age, placing an upper limit on LGM thickening at ~655 m. One sample from Mt. Skidmore, collected from ~284 m asl, yields an infinite age. Above the saturated sample we observe seven finite-aged samples which require significant periods of burial beneath ice to account for their in situ ^{14}C concentrations. It is glaciologically impossible to have the sample at ~284 m asl exposed for ca. 35 kyr whilst those above it were covered presumably by the Slessor and Stratton glaciers. The infinite age of the sample could be due to scatter within the ^{14}C measurements, and the fact that the sample is an erratic does allow the possibility of an unlikely geomorphic scenario. As described in Sect. 1.2, erratic samples may be sourced from mass movement onto glacier surfaces, producing spuriously high ^{14}C concentrations (Balco et al., accepted).

On the Lassiter Coast, Johnson et al. (in review) report ^{10}Be ages which, with the exception of three measurements, all exceed ~100 ka, whilst all of the in situ ^{14}C ages are finite and fall within the Holocene (Fig. 6). The associated in situ ^{14}C concentrations are similar over the range of sample elevations (Fig. 6). The uppermost sample, collected ~385 m above the modern ice surface, provides a lower limit on the thickness of LGM ice at the Lassiter Coast. The small range of ages across ca. 300 m elevation transect indicate that deglaciation occurred rapidly at this study site (Johnson et al. in review).

At the Schmidt Hills, ^{10}Be ages from Balco et al. (2016) and Bentley et al. (2017) range from ~140 ka to 3 Ma (Fig. 7). We observe finite ages at low elevations and finite, close to infinite, and infinite ages at higher elevations (Fig. 7). Given that higher elevations cannot be covered by ice unless lower elevations were also covered, we remeasured the apparently infinite and near-infinite aged samples (~500 to ~920 m asl, or ~270 to ~690 m above the modern ice surface). The replicate results (Fig. 7) show high variability, greater than that observed in previous repeat measurements of CRONUS-A and other samples (Goehring et al., 2019). There is no apparent analytical reason for the initial measurements yielding infinite or near-infinite ages and then yielding differing concentrations with repeat measurements. Samples yielding only finite ages (those that were not measured multiple times) are observed up to ~420 m asl, or ~190 m above the modern ice surface. In addition, the bedrock sample collected from ca. 1035 m asl yields a finite age, indicating at least ~800 m of LGM thickening of the FIS at the Schmidt Hills. The agreement between the bedrock age and the finite measurements from lower elevations means we conclude that 800 m of LGM thickening occurred at the Schmidt Hills. This conclusion, and the repeat measurements with a high degree of scatter, are discussed in Sect. 4.1 and 4.2.

The two samples collected from the Thomas Hills yield finite ages within ~0.2 ka of one another (Fig. 8). Results thus indicate a minimum of ~320 m of LGM thickening at the Thomas Hills. The apparent in situ ^{14}C ages, at ~10 ka, are consistent with a cluster of ^{10}Be ages between 7 and 9 ka in the Thomas Hills reported by Balco et al. (2016) from 225 m above the modern FIS surface, as well as a ^{10}Be age of 4.2 ka reported by Bentley et al. (2017) collected 125 m above the modern ice surface. Considering the evidence for significant LGM thickening of the FIS from our in situ ^{14}C results from the Thomas Hills, as well as ^{10}Be ages of Balco et al. (2016) and Bentley et al. (2017) from both the Williams and Thomas Hills, we conclude that it is likely that the FIS reached up to 800 m above its present thickness at the LGM at the Schmidt Hills. We discuss this conclusion further in the following section.

4.0 Discussion

4.1. Assessment of ^{14}C elevation transects

The premise of our study is that one can clearly infer if a site was ice-covered at the LGM by determining whether the in-situ ^{14}C concentration of samples from that site are at or below saturation. Here we assess the success of this approach. At some sites our results are consistent with the premise, as well as internally consistent. At the Lassiter Coast we observe a linear age-elevation relation in the finite ages. Though limited by the number of samples, two measurements from Mt. Provender align with the premise of our study, in that we find a finite age located at a low elevation with an infinite age above it. In the Thomas Hills we see consistency between the finite ^{14}C ages and previously-published ^{10}Be ages (Balco et

al., 2016; Bentley et al., 2017). Fogwill et al. (2014) also observe consistency between ^{14}C and ^{10}Be ages, which constrain the LGM thickness and dynamics of the Rutford Ice Stream. However, we observe apparently finite ages above apparently infinite ages at the Schmidt Hills, a scenario that is glaciologically impossible if our assumptions are correct that samples are indeed glacial erratics that have either been deposited previously and repeatedly covered by cold-based ice or delivered to their sampling location during the last glaciation and were sourced subglacially. The scatter observed in the repeat measurements (Fig. 7) is greater than that of repeat measurements made of CRONUS-A and other samples made in our laboratory (Goehring et al., 2019). Three samples from the Schmidt Hills (006-COU, 008-NNS and 046-NNS, collected from ~920, ~710 and ~500 m asl, respectively) were previously measured for their in situ ^{14}C content (Balco et al., 2016). All three of the samples previously measured yielded higher concentrations than the new measurements, two of which were above saturation with the third at saturation. Furthermore, two of the three samples (006-COU and 046-NNS) were measured multiple times and display the high scatter under discussion. Balco et al. (2016) proposed unrecognised measurement error as the cause of the spuriously high in situ ^{14}C concentrations. Why the high degree of scatter displayed in replicate measurements seems to be exclusive to the Schmidt Hills remains to be determined.

Regardless, for the purposes of this work we need to discuss possible explanations for apparently infinite ages at lower elevations than apparently finite ages. At the Schmidt Hills, the hypothesis that infinite ages situated below finite ages are spurious and due to measurement errors is consistent with the glaciological relationship amongst the Schmidt, Thomas and Williams Hills, shown in Fig. 10, and is also consistent with the finite bedrock age sourced from a higher elevation. The bedrock age is a robust constraint because the sample cannot have been subjected to geomorphic scenarios that could cause the resulting age to misrepresent the timing of deglaciation. The hypothesis that the infinite ages are correct produces a steep LGM surface slope and is not consistent with thickness estimates from the Williams and Thomas Hills. We elaborate on this point in Sect. 4.2.

As described in Sect. 1.2, it is theoretically possible for in situ ^{14}C saturated samples to occur at lower elevations than finite ages in rare situations if the former were transported by LGM ice. Balco et al. (accepted) observed an apparently saturated sample beneath finite aged samples. Supported by field observations, Balco et al. (accepted) propose that the saturated sample was sourced from a rockfall upstream and transported to the study site as supraglacial debris, explaining the elevated in situ ^{14}C concentration. This is possible, if unlikely, with our Schmidt Hills samples, given that all of the measurements in question are taken from erratic cobbles sourced from upstream of the Schmidt Hills (Balco et al., 2016).

The most likely reason for ^{14}C measurement error is contamination by modern ^{14}C, which would result in a spuriously high concentration. In contrast, a spuriously low concentration is less likely, and we are not aware of any documented instances of this. In our laboratory we have found that it is relatively easy to contaminate a sample with ^{14}C, for example through the use of organic compounds in the froth flotation mineral separation procedure (Nichols et al., in preparation). However, froth flotation was not used to isolate the quartz of any of the samples for which replicate measurements were made. On multiple occasions we have observed spuriously high ^{14}C concentrations, far in excess of saturation concentrations, from quartz separates of fine grain sizes (ca. 60 µm). Perhaps the finite-aged replicate measurements were unintentionally made using quartz separates with a higher average grain size than the initial infinite measurements. We believe the above observations indicate that the increased scatter may be the result of measurement difficulties, perhaps lithology- or grain size-specific.

We conclude that the basic concept works, as shown at the Lassiter Coast and the Shackleton Range, as well as in other aforementioned studies. In the following section we discuss the implications for LGM ice sheet reconstructions. However, it is clear that more investigation into laboratory issues, geological and geomorphic factors is required to identify the cause or causes of apparently site- or lithology-specific excess scatter in in situ ^{14}C measurements.

4.2 LGM ice thicknesses in the Weddell Sea Embayment

The new in situ ^{14}C concentrations indicate that the entirety of Mt. Skidmore, and presumably much of Mt. Provender, was covered by ice at the LGM (Figs. 5 and 9). The highest elevation samples on Mt. Skidmore proximal to the ice stream suggest that at least 300 m of LGM thickening occurred at Mt. Skidmore. This assumes the samples were not influenced by expansion of local ice masses from the southeast (Fig. S1) If so, and assuming the surface gradient of Slessor Glacier during the LGM was similar to today, this would suggest ~300 m thickening also occurred at Mt. Provender. With no

high-elevation infinite ages found on Mt. Skidmore, our thickness estimates for the Slessor Glacier are likely conservative estimates. Our data indicate that, regardless of the source, the Mt. Skidmore site was covered by ice during the LGM, whilst the top of Mt. Provender remained exposed. Our thickness constraints (~300-650m) supersede those of previous exposure dating studies that found no evidence from long-lived isotopes for a thicker Slessor Glacier at the LGM (Hein et al, 2011; 2014). Our LGM thickness constraints for the Slessor Glacier are consistent with our other sites as well as those of previous authors for a significantly thicker FIS at the LGM (Balco et al., 2016; Bentley et al., 2017).

The new in situ ^{14}C results from the Lassiter Coast show that bedrock surfaces 385 m above the modern ice surface were covered by ice at the LGM. As with results in the Pensacola Mountains, with only a lower limit for LGM thickening of 360 m, there could have been thicker ice on the Lassiter Coast at the LGM. The in situ ^{14}C measurements contrast with ^{10}Be measurements that were likely influenced by cold-based ice cover, resulting in nuclide inheritance (Johnson et al., in review). The finite in situ ^{14}C ages are consistent with a minimum age of grounded ice retreat from a marine sediment core close to the modern ice shelf edge of 5.3 ± 0.3 kcal yr BP (Hedges et al., 1995; Crawford et al., 1996; Fig. 1). The fact that significant thinning occurred in the Holocene may help explain the misfit between GIA models and GPS measurements in Palmer Land (Wolstencroft et al., 2015). A thicker ice load at the LGM than that used by current ice models, or present ice load estimates that persist into the Holocene, are two potential solutions postulated by Wolstencroft et al. (2015) to explain the misfit. Further work is needed to take our new ice history into account and to investigate if a minimum of 385 m of ice at the LGM and subsequent rapid thinning at ~7 ka at the Lassiter Coast can help account for the offset.

Our in situ ^{14}C data indicate that the FIS was at least 800 m thicker than present at the LGM at the Schmidt Hills, which contrasts with previous studies which found no evidence for LGM thickening of the FIS at the Schmidt Hills (Balco et al., 2016; Bentley et al., 2017). We base our LGM thickness estimate on the aforementioned finite-aged repeat measurements and the finite aged bedrock sample, rather than on the poorly reproduced infinite aged-measurements. There is robust evidence for at least 500 m of LGM thickening at the Williams Hills, located only 50 km upstream of the Schmidt Hills (Figs. 1 and 10; Balco et al., 2016; Bentley et al., 2017). Given the evidence for significant thickening proximal to the Schmidt Hills, we argue that the repeat measurements and the bedrock measurement indicative of 800 m of thickening of the FIS are glaciologically most-likely, and thus base our LGM ice thickness estimates on them. Using the infinite measurements and accompanying estimate of 320 m LGM thickening at the Schmidt Hills produces a steep surface slope from the nearby Williams Hills (Fig. 10), though less so than the surface slope produced when no LGM thickening is inferred at the Schmidt Hills based on ^{10}Be measurements (Balco et al., 2016). The two measurements from the Thomas Hills provide a lower limit for LGM thickening, but the possibility remains that there was more thickening than the ca. 320 m in situ ^{14}C constraint. Fig. 10 tentatively suggests that there may have been ~900 m of thickening when using the modern surface profile of the FIS increased in elevation up to the height of the finite ages from the Schmidt Hills and post-12ka ^{10}Be ages from Balco et al. (2016) and Bentley et al. (2017) from the Williams Hills. This is a tentative interpretation because, if thickening is sea level controlled, there would be progressively less thinning expected upstream.

Our LGM ice thickness constraints are consistent with evidence for significant LGM thickening in the Ellsworth Mountains (Hein et al., 2016, Fig. 2), and also likely consistent with measurements in Bentley et al. (2006). The post-LGM exposure ages of Hein et al. (2016) constrain LGM thickening to between 475, 373 and 247 m at three study sites in the Ellsworth Mountains. A pulse of up to 410 m of thinning appears similar both in scale and timing to the rapid ice surface lowering of 385 m recorded at the Lassiter Coast. Furthermore, measurements of long-lived nuclides by Bentley et al. (2006) show that there has been at least 300 m of thinning since the LGM in the Behrendt Mountains (Bentley et al., 2006).

4.3 Grounding line position and flowline modelling comparison

Whitehouse et al. (2017) use their flowline model to reproduce the modern FIS ice surface profile and investigate the response of the ice stream to the onset of glacial and interglacial conditions. The following results from Whitehouse et al. (2017) are from their experiments in which the FIS is routed to the east of Berkner Island, which it is believed to have done during the LGM based on modelling studies (Le Brocq et al., 2011; Whitehouse et al., 2012) and aforementioned marine

geological evidence for the former presence of grounded ice (Sect. 1.1). Under glacial conditions the FIS thickens by 299 to 494 m adjacent to the Thomas Hills, 231 to 422 m adjacent to the Williams Hills, 156 to 337 m adjacent to the Schmidt Hills, and 113 to 285 m proximal to the Shackleton Range. The lower value for each location is sourced from flowline experiments during which the grounding line of the FIS reaches a stable position at the northern margin of Berkner Island, with the higher value sourced from a scenario during which the grounded ice stream stabilises at the offshore shelf edge. Our in situ ^{14}C LGM thickness constraints at each study location in the Pensacola Mountains and Shackleton Range exceed the upper estimates of the FIS flowline model of Whitehouse et al. (2017) under glacial conditions. The flowline model shows that the FIS, a major contributor to the total WSE ice flux, is able to reach a stable position at the offshore shelf edge when tuned using LGM thickness constraints lower than those presented here. Therefore, our thickness estimates add strength to the hypothesis that grounded ice occupying the WSE during the LGM reached a stable position located at the offshore shelf edge (Bentley and Anderson, 1998; Hillenbrand et al., 2014).

4.4 Sea-Level contribution

We use a highly simplified scenario in which a range of LGM thickness change estimates are distributed evenly across the WSE using an area for the sector defined by Hillenbrand et al (2014). Distributing the lowest of our LGM thickness estimates, 310 m for the Slessor Glacier, over the entire WSE produces a sea-level equivalent (SLE) of 2.2 m. When using the highest of our thickness estimates, 800 m for the FIS, the SLE increases to 5.8 m. Using the average LGM thickness constraint for our three study sites (580 m) produces a SLE for the sector of 4.2 m. This scenario lacks any glaciological basis and is unrealistic, with no variation in ice thickness with location and no consideration of ice dynamics, isostasy, or bathymetry, thus further work is required to produce a realistic SLE for the WSE using our in situ ^{14}C thickness constraints. However, despite being rough estimates, our SLE values are comparable to those modelled by Bentley et al. (2010) (1.4 m to 2 m) and Le Brocq et al. (2011) (1.4 to 3 m), but much lower than the estimate of Bassett et al. (2007) (13.1 to 14.1 m). Our exposure ages indicate the Weddell Sea contributed to sea-level most significantly during the early to mid-Holocene, though they do not preclude a significant contribution earlier than this. The majority of the exposure ages post-date Meltwater Pulse 1A (MWP1A) (~14.6 ka, Carlson and Clark et al., 2012), thus it appears unlikely that the sector contributed significantly to the rapid rise in sea-level. There doesn't seem to be a sufficient volume of ice in the WSE at the LGM to account for a significant contribution to any rapid rises in sea-level, though many of our ice thickness constraints only provide lower limits and thus do not rule out significant ice loss prior to our oldest exposure ages. Nevertheless, our estimates imply that the sector provided a modest contribution to global sea-level. Whitehouse et al. (2017) estimate the sea-level contribution of the FIS to between ~0.05 and ~0.13 m. Given that our ^{14}C thickness constraints for the FIS, including those in the Shackleton Range, exceed all of those used by Whitehouse et al. (2017) to tune their flowline model, we propose that the sea-level contribution for the FIS was greater than their upper estimate of ~0.13 m.

5. Conclusions

This study presents LGM ice thickness constraints for three locations within the WSE of Antarctica. In situ ^{14}C measurements constrain LGM thickening of the FIS to at least ca. 800 m in the Schmidt Hills and at least 320 m in the Thomas Hills, both in the Pensacola Mountains. The Slessor Glacier was at least 310 m and up to 655 m thicker than present at the LGM. Finally, LGM ice was at least 360 m thicker than present at the Lassiter Coast. Our thickness constraints resolve a significant disconnect between previous terrestrial evidence for minimal LGM thickening in some locations from long-lived nuclides, and marine evidence for a significantly laterally expanded ice sheet with the grounding line located at the offshore shelf edge. Given that the majority of the in situ ^{14}C exposure ages post-date the rapid rise in sea-level, it seems unlikely that the WSE contributed significantly to MWP1A. In terms of the total contribution of the ice sheet sector to global sea-level rise since the LGM, we estimate that the WSE contributed modestly, with a rough estimate of between 2.2 and 5.8 m if 310 to 800 m of vertical thickening is distributed equally across the sector.

Data availability

All sample data, including photographs when available, are available in the Informal Cosmogenic-Nuclide Exposure-Age Database (ICE-D) (http://antarctica.ice-d.org).

Author contributions

The study was conceived by BM and GB. Sample material was originally collected and provided by AH, JJ, GB, and CT. Sample preparation and analysis undertaken by KN and BM. Manuscript was written by KN with help from all authors.

Competing interests:

The authors declare that they have no conflict of interest.

Acknowledgements

KN and BG acknowledge support NSF-OPP grant 1542936. Geospatial support for this work provided by the Polar Geospatial Center under NSF-OPP awards 1043681 and 1559691. This work forms part of the British Antarctic Survey 'Polar Science for Planet Earth' programme, funded by the Natural Environment Research Council.

References

Note - Added two references that were omitted in the initial file submission (Huybers, 2014; Johnson et al., in review).

Ackert, R. P., Mukhopadhyay, S., Parizek, B. R. and Borns, H. W.: Ice elevation near the West Antarctic Ice Sheet divide during the Last Glaciation, Geophys. Res. Lett., 34(21), 1–6, doi:10.1029/2007GL031412, 2007.

Arndt, J. E., Schenke, H. W., Jakobsson, M., Nitsche, F. O., Buys, G., Goleby, B., Rebesco, M., Bohoyo, F., Hong, J., Black, J., Greku, R., Udintsev, G., Barrios, F., Reynoso-Peralta, W., Taisei, M. and Wigley, R.: The international bathymetric chart of the Southern Ocean (IBCSO) version 1.0-A new bathymetric compilation covering circum-Antarctic waters, Geophys. Res. Lett., 40(12), 3111–3117, doi:10.1002/grl.50413, 2013.

Arndt, J. E., Hillenbrand, C.-D., Grobe, H., Kuhn, G. and Wacker, L.: Evidence for a dynamic grounding line in outer Filchner Trough, Antarctica, until the early Holocene, Geology, 45(11), 1035–1038, doi:10.1130/G39398.1, 2017.

Balco, G., Stone, J. O., Lifton, N. A. and Dunai, T. J.: A complete and easily accessible means of calculating surface exposure ages or erosion rates from 10Be and 26Al measurements, Quat. Geochronol., 3(3), 174–195, doi:10.1016/j.quageo.2007.12.001, 2008.

Balco, G., Todd, C., Huybers, K., Campbell, S., Vermeulen, M., Hegland, M., Goehring, B. M. and Hillebrand, T. R.: Cosmogenic-nuclide exposure ages from the Pensacola Mountains adjacent to the foundation ice stream, Antarctica, Am. J. Sci., 316(6), 542–577, doi:10.2475/06.2016.02, 2016.

Balco, G., Todd, C., Goehring, B.M., Moening-Swanson, I., Nichols, K. Glacial geology and cosmogenic-nuclide exposure ages from the Tucker Glacier-Whitehall Glacier confluence, northern Victoria Land, Antarctica, Am. J. Sci, Accepted.

Bassett, S. E., Milne, G. A., Bentley, M. J. and Huybrechts, P.: Modelling Antarctic sea-level data to explore the possibility of a dominant Antarctic contribution to meltwater pulse IA, Quat. Sci. Rev., 26(17–18), 2113–2127, doi:10.1016/j.quascirev.2007.06.011, 2007.

Bentley, M. J. and Anderson, J. B.: Glacial and marine geological evidence for the ice sheet configuration in the Weddell Sea–Antarctic Peninsula region during the Last Glacial Maximum, Antarct. Sci., 10(3), 309–325, doi:10.1017/s0954102098000388, 1998.

Bentley, M. J., Fogwill, C. J., Kubik, P. W. and Sugden, D. E.: Geomorphological evidence and cosmogenic 10Be/26Al exposure ages for the Last Glacial Maximum and deglaciation of the Antarctic Peninsula Ice Sheet, Bull. Geol. Soc. Am., 118(9–10), 1149–1159, doi:10.1130/B25735.1, 2006.

Bentley, M. J., Fogwill, C. J., Brocq, A. M. Le, Hubbard, A. L., Sugden, D. E., Dunai, T. J. and Freeman, S. P. H. T.: Deglacial history of the West Antarctic Ice Sheet in the Weddell Sea embayment: Constraints on past ice volume change, Geol. Soc. Am., 38(5), 411–414, doi:10.1130/G30754.1, 2010.

Bentley, M. J., Hein, A. S., Sugden, D. E., Whitehouse, P. L., Shanks, R., Xu, S. and Freeman, S. P. H. T.: Deglacial history of the Pensacola Mountains, Antarctica from glacial geomorphology and cosmogenic nuclide surface exposure dating, Quat. Sci. Rev., 158, 58–76, doi:10.1016/j.quascirev.2016.09.028, 2017.

Briggs, R. D., Pollard, D. and Tarasov, L.: A data-constrained large ensemble analysis of Antarctic evolution since the Eemian, Quat. Sci. Rev., 103, 91–115, doi:10.1016/j.quascirev.2014.09.003, 2014.

Le Brocq, A. M., Bentley, M. J., Hubbard, A., Fogwill, C. J., Sugden, D. E. and Whitehouse, P. L.: Reconstructing the Last Glacial Maximum ice sheet in the Weddell Sea embayment, Antarctica, using numerical modelling constrained by field evidence, Quat. Sci. Rev., 30(19–20), 2422–2432, doi:10.1016/j.quascirev.2011.05.009, 2011.

Carlson, Anders E; Clark, P. U.: Ice sheet sources of sea level rise and freshwater discharge during the last deglaciation, Rev. Geophys., 50, 1–72, doi:10.1029/2011RG000371, 2012.

Crawford, K., Kuhn, G. and Hambrey, M.: Changes in the character of glaciomarine sedimentation in the southwestern Weddell Sea, Antarctica: evidence from the core PS1423-2, Ann. Glaciol., 22, 200–204 [online] Available from: http://epic.awi.de/554/1/Cra1996a.pdf, 1996.

Fogwill, C. J., Bentley, M. J., Sugden, D. E., Kerr, A. R. and Kubik, P. W.: Cosmogenic nuclides 10Be and 26Al imply limited Antarctic Ice Sheet thickening and low erosion in the Shackleton Range for >1 m.y, Geology, 32(3), 265–268, doi:10.1130/G19795.1, 2004.

Goehring, B. M., Wilson, J. and Nichols, K.: A fully automated system for the extraction of in situ cosmogenic carbon-14 in the Tulane University cosmogenic nuclide laboratory, Nucl. Instruments Methods Phys. Res. Sect. B Beam Interact. with Mater. Atoms, doi:10.1016/j.nimb.2019.02.006, 2019.

Hedges, R. E. M., Housley, R. A., Ramsey, C. B. and Van Klinken, G. J.: Radiocarbon Dates from the Oxford AMS System: Archaeometry Datelist 19, Archaeometry, 37(1), 195–214, 1995.

Hein, A. S., Fogwill, C. J., Sugden, D. E. and Xu, S.: Glacial/interglacial ice-stream stability in the Weddell Sea embayment, Antarctica, Earth Planet. Sci. Lett., 307(1–2), 211–221, doi:10.1016/j.epsl.2011.04.037, 2011.

Hein, A. S., Fogwill, C. J., Sugden, D. E. and Xu, S.: Geological scatter of cosmogenic-nuclide exposure ages in the Shackleton Range, Antarctica: Implications for glacial history, Quat. Geochronol., 19, 52–66, doi:10.1016/j.quageo.2013.03.008, 2014.

Hein, A. S., Marrero, S. M., Woodward, J., Dunning, S. A., Winter, K., Westoby, M. J., Freeman, S. P. H. T., Shanks, R. P. and Sugden, D. E.: Mid-Holocene pulse of thinning in the Weddell Sea sector of the West Antarctic ice sheet, Nat. Commun., 7, 1–8, doi:10.1038/ncomms12511, 2016.

Herber, L. J.: Separation of feldspar from quartz by flotation, Am. Mineral., 54, 1212–1215, doi:10.4144/rpsj1954.25.192, 1969.

Hillenbrand, C. D., Melles, M., Kuhn, G. and Larter, R. D.: Marine geological constraints for the grounding-line position of the Antarctic Ice Sheet on the southern Weddell Sea shelf at the Last Glacial Maximum, Quat. Sci. Rev., 32, 25–47, doi:10.1016/j.quascirev.2011.11.017, 2012.

Hillenbrand, C. D., Bentley, M. J., Stolldorf, T. D., Hein, A. S., Kuhn, G., Graham, A. G. C., Fogwill, C. J., Kristoffersen, Y., Smith, J. A., Anderson, J. B., Larter, R. D., Melles, M., Hodgson, D. A., Mulvaney, R. and Sugden, D. E.: Reconstruction of changes in the Weddell Sea sector of the Antarctic Ice Sheet since the Last Glacial Maximum, Quat. Sci. Rev., 100, 111–136, doi:10.1016/j.quascirev.2013.07.020, 2014.

Hodgson, D. A., Bentley, M. J., Schnabel, C., Cziferszky, A., Fretwell, P., Convey, P. and Xu, S.: Glacial geomorphology and cosmogenic 10 Be and 26 Al exposure ages in the northern Dufek Massif, Weddell Sea embayment, Antarctica, Antarct. Sci., 24(4), 377–394, doi:10.1017/S0954102012000016, 2012.

Howat, I. M., Porter, C., Smith, B. E., Noh, M.-J. and Morin, P.: The Reference Elevation Model of Antarctica, Cryosph. Discuss., 13, 1–16, doi:10.5194/tc-2018-240, 2019.

Huybers, K.: Relationships between climate and geophysical processes: what climate histories can be inferred from glaciers, lakes, and ice streams?, 2014.

Johnson, J., Nichols, K.A., Goehring, B.M., Balco, G., Schaefer, J.: Abrupt mid-Holocene ice loss in the western Weddell Sea Embayment of Antarctica, Earth Planet. Sci. Lett., In review

Joughin, I., Bamber, J. L., Scambos, T., Tulaczyk, S., Fahnestock, M. and MacAyeal, D. R.: Integrating satellite observations with modelling: Basal shear stress of the Filcher-Ronne ice streams, Antarctica, Philos. Trans. R. Soc. A Math. Phys. Eng. Sci., 364(1844), 1795–1814, doi:10.1098/rsta.2006.1799, 2006.

Jull, A. J. T., Scott, E. M. and Bierman, P.: The CRONUS-Earth inter-comparison for cosmogenic isotope analysis, Quat. Geochronol., 26(1), 3–10, doi:10.1016/j.quageo.2013.09.003, 2015.

Larter, R. D., Graham, A. G. C., Hillenbrand, C.-D., Smith, J. A. and Gales, J. A.: Late Quaternary grounded ice extent in the Filchner Trough, Weddell Sea, Antarctica: New marine geophysical evidence, Quat. Sci. Rev., 53(C), 111–122, doi:10.1016/j.quascirev.2012.08.006, 2012.

Lifton, N., Sato, T. and Dunai, T. J.: Scaling in situ cosmogenic nuclide production rates using analytical approximations to atmospheric cosmic-ray fluxes, Earth Planet. Sci. Lett., 386, 149–160, doi:10.1016/j.epsl.2013.10.052, 2014.

Nichols, K., Goehring, B.: Isolation of quartz for cosmogenic in situ 14C analysis. In preparation.

Pollard, D., Chang, W., Haran, M., Applegate, P. and DeConto, R.: Large ensemble modeling of the last deglacial retreat of the West Antarctic Ice Sheet: Comparison of simple and advanced statistical techniques, Geosci. Model Dev., 9(5), 1697–1723, doi:10.5194/gmd-9-1697-2016, 2016.

Pollard, D., Gomez, N. and Deconto, R. M.: Variations of the Antarctic Ice Sheet in a Coupled Ice Sheet-Earth-Sea Level Model: Sensitivity to Viscoelastic Earth Properties, J. Geophys. Res. Earth Surf., 122(11), 2124–2138, doi:10.1002/2017JF004371, 2017.

Rignot, E., Mouginot, J. and Scheuchl, B.: Antarctic grounding line mapping from differential satellite radar interferometry, Geophys. Res. Lett., 38, 1–6, doi:10.1029/2011GL047109, 2011.

Rignot, E., Mouginot, J., Morlighem, M., Seroussi, H. and Scheuchl, B.: Widespread, rapid grounding line retreat of Pine Island, Thwaites, Smith, and Kohler glaciers, West Antarctica, from 1992 to 2011, Geophys. Res. Lett., 41, 3502–3509, doi:10.1002/2014GL060140, 2014.

Rignot, E., J. Mouginot, and B. Scheuchl.: MEaSUREs Antarctic Grounding Line from Differential Satellite Radar Interferometry, Version 2, [All subsets], NASA National Snow and Ice Data Center Distributed Active Archive Center, https://doi.org/10.5067/IKBWW4RYHF1Q, [Accessed 9th January 2019], 2016.

Simms, A. R., Lisiecki, L., Gebbie, G., Whitehouse, P. L. and Clark, J. F.: Balancing the last glacial maximum (LGM) sea-level budget, Quat. Sci. Rev., 205, 143–153, doi:10.1016/j.quascirev.2018.12.018, 2019.

Stone, J. O., Balco, G. A., Sugden, D. E., Caffee, M. W., Sass, L. C., Cowdery, S. G. and Siddoway, C.: Holocene deglaciation of Marie Byrd Land, West Antarctica, Science (80-.)., 299(5603), 99–102, doi:10.1126/science.1077998, 2003.

Sugden, D. E., Balco, G., Sass, L. C., Cowdery, S. G. and Stone, J. O.: Selective glacial erosion and weathering zones in the coastal mountains of Marie Byrd Land, Antarctica, Geomorphology, 67(3–4), 317–334, doi:10.1016/j.geomorph.2004.10.007, 2005.

Sugden, D. E., Hein, A. S., Woodward, J., Marrero, S. M., Rodes, A., Dunning, S. A., Stuart, F. M., Freeman, S. P. H. T., Winter, K. and Westoby, M. J.: The million-year evolution of the glacial trimline in the southernmost Ellsworth Mountains, Antarctica, Earth Planet. Sci. Lett., 469, 42–52, doi:10.1016/j.epsl.2017.04.006, 2017.

Whitehouse, P. L., Bentley, M. J. and Le Brocq, A. M.: A deglacial model for Antarctica: Geological constraints and glaciological modelling as a basis for a new model of Antarctic glacial isostatic adjustment, Quat. Sci. Rev., 32, 1–24, doi:10.1016/j.quascirev.2011.11.016, 2012.

Whitehouse, P. L., Bentley, M. J., Vieli, A., Jamieson, S. S. R., Hein, A. S. and Sugden, D. E.: Controls on Last Glacial Maximum ice extent in the Weddell Sea embayment, Antarctica, J. Geophys. Res. Earth Surf., 122(1), 371–397, doi:10.1002/2016JF004121, 2017.

Wolstencroft, M., King, M. A., Whitehouse, P. L., Bentley, M. J., Nield, G. A., King, E. C., McMillan, M., Shepherd, A., Barletta, V., Bordoni, A., Riva, R. E. M., Didova, O. and Gunter, B. C.: Uplift rates from a new high-density GPS network in Palmer Land indicate significant late Holocene ice loss in the southwestern Weddell Sea, Geophys. J. Int., 203(1), 737–754, doi:10.1093/gji/ggv327, 2015.

Figures

Figure 1: The Weddell Sea Embayment, including all locations referred to within the text. SH, WH and TH are the Schmidt, Williams and Thomas Hills, respectively. FH, P/M and MH are the Flower Hills, Patriot and Marble Hills, and the Meyer Hills, respectively. Black is exposed rock. Red boxes show extent of satellite images in Fig. 4. Exposed rock and coastline sourced from the SCAR Antarctic Digital Database. Bathymetry sourced from the International Bathymetric Chart of the Southern Ocean V1.0 (IBSCO; Arndt et al., 2013). Surface topography (shading) is sourced from the Reference Elevation Model of Antarctica (REMA; Howat et al., 2019). PS1423-2 is a marine sediment core from Crawford et al. (1996).

Figure 2: Current terrestrial constraints Ice thickness constraints inferred from measurements of long-lived nuclides around the WSE. Acronyms are as in Fig. 1. Constraints for the SH, WH, and TH are sourced from Balco et al. (2016) and Bentley et al. (2017). MB is Mount Bragg (Bentley et al., 2017). Thickness estimate for the Dufek Massif (DM) is sourced from Hodgson et al. (2012). Constraints for the P/M are sourced from Hein et al. (2016). For the MH and FH, the LGM thickness constraints are sourced from Fogwill et al. (2014). The thickness constraints sourced from Fogwill et al. (2014) were interpreted using modern ice surface elevations for the Rutford Ice Stream and Union Glacier measured using the Reference Elevation Model of Antarctica (REMA;Howat et al., 2019). Thickness constraints for the Shackleton Range are sourced from Hein et al. (2011; 2014). The range of LGM thicknesses for the Behrendt Mountains are sourced from multiple locations (Bentley et al., 2006).

Figure 3: Left: Hypothetical ice surface elevation change at a nunatak partially covered by ice at the LGM. Right: Resulting in situ 14C concentration in samples collected at 100 m intervals along an elevation transect on the surface of the nunatak. Thin black lines indicate isochrons of exposure duration. Thick black line with dashed lines either side represent the saturation concentration and associated error envelope. “True exposure” refers to the true exposure age associated with the ice surface change history on the left plot. “Apparent exposure” is the resulting concentration that includes an inherited component, which is a residual 14C inventory remaining from the hypothetical samples which were saturated prior to ice cover.

Figure 4: Landsat imagery of study sites. Location of each image is shown in Fig. 1. Green dots show sample locations. Arrows show ice flow directions. A: Mt. Skidmore and Mt. Provender, Shackleton Range. B: Lassiter Coast, southern Palmer Land. C: Schmidt Hills, Pensacola Mountains. D: Thomas Hills, Pensacola Mountains. Landsat 8 imagery courtesy of the U.S. Geological Survey. Grounding line positions sourced from the MEaSUREs program V2 (Rignot et al., 2011; 2014; 2016).

Figure 5: Left: Elevation versus in situ 14C concentration of samples from the Shackleton Range. Circles are erratic cobbles, triangles are bedrock. Some error bars are smaller than their respective data points. Horizontal dashed lines show the approximate elevation of the modern ice surface at each site. Light grey lines indicate isochrons of exposure duration. Thick black line and two lines either side are the saturation concentration and associated error envelope. Right: Exposure ages from this study (in situ 14C) and 10Be ages of Hein et al. (2011; 2014). Samples yielding infinite in situ 14C ages are not presented on the right-hand plot.

Figure 6: Left: Elevation versus in situ ^{14}C concentration of samples collected from the Lassiter Coast. All samples are bedrock. Right: In situ 14C exposure ages with ^{10}Be ages of Johnson et al. (in review).

Figure 7: Left: Elevation versus in situ ^{14}C concentration of samples collected from the Schmidt Hills. All samples are erratics with the exception of the highest elevation sample, shown with a triangle. Samples with replicate measurements are displayed with differing symbols. Right: Schmidt Hills exposure ages from this study (in situ ^{14}C) and those of Balco et al. (2016) and Bentley et al. (2017) (^{10}Be). Measurements yielding infinite in situ ^{14}C ages are not presented on the right-hand plot.

Figure 8: Left: Elevation versus in situ ^{14}C concentration of samples collected from the Thomas Hills. All samples are erratics. Note that both plots contain in situ 14C data for two samples within close agreement, such that the points overlap. Right: Thomas Hills exposure ages from this study (in situ ^{14}C) and those of Balco et al. (2016) and Bentley et al. (2017) (^{10}Be).

Figure 9: Exposure-age results projected onto an elevation profile along flowline of the Slessor Glacier. Flowline location is shown in the map (left). Infinite ^{14}C measurements are offset in regard to their distance along flowline to improve readability. The ^{10}Be data included are those from Hein et al. (2011; 2014) which yield exposure ages below 12 ka (LSDn scaling, antarctica.ice-d.org). Elevation data for ice surfaces and map shading is sourced from the Reference Elevation Model of Antarctica (REMA; Howat et al., 2018). Grounding zone positions sourced from the MEaSUREs program V2 (Rignot et al., 2011; 2014; 2016). Minimum LGM surface is the modern day surface profile with the elevation increased above present using our minimum LGM thickness estimates.

Figure 10: Exposure-age results projected onto an elevation profile along flowline of the Foundation Ice Stream. Flowline location is shown in the map (left). Infinite ^{14}C measurements are offset in regard to their distance along flowline to improve readability. The ^{10}Be data included are those from Balco et al. (2016) and Bentley et al. (2017) which yield exposure ages below 12 ka (LSDn scaling, antarctica.ice-d.org). Elevation data for ice surfaces and map shading is sourced from the Reference Elevation Model of Antarctica (REMA;Howat et al., 2019). Local ice margins are highly simplified. Grounding zone positions are sourced from the MEaSUREs program V2 (Rignot et al., 2011; 2014; 2016)). Minimum LGM surface is the modern day surface profile with the elevation increased above present using our minimum LGM thickness estimates.

The Cryosphere Discuss., https://doi.org/10.5194/tc-2019-64
Manuscript under review for journal The Cryosphere
Discussion started: 14 May 2019

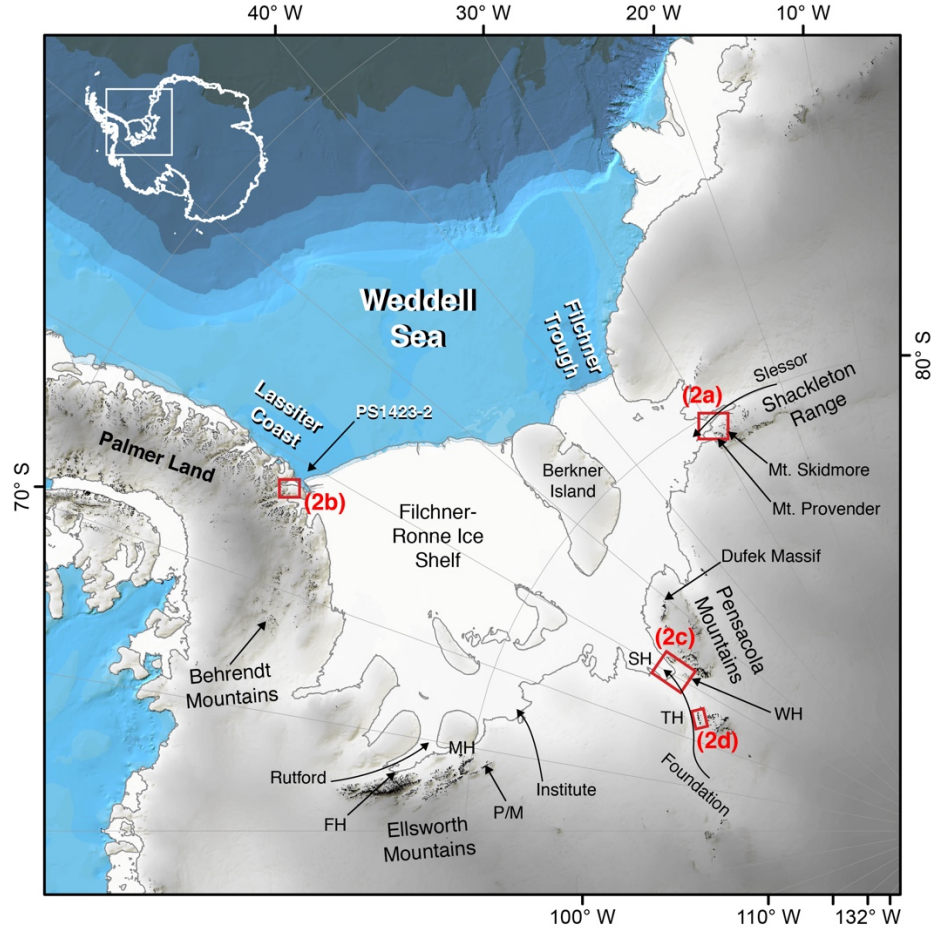

Fig. 1

The Cryosphere Discuss., https://doi.org/10.5194/tc-2019-64
Manuscript under review for journal The Cryosphere
Discussion started: 14 May 2019

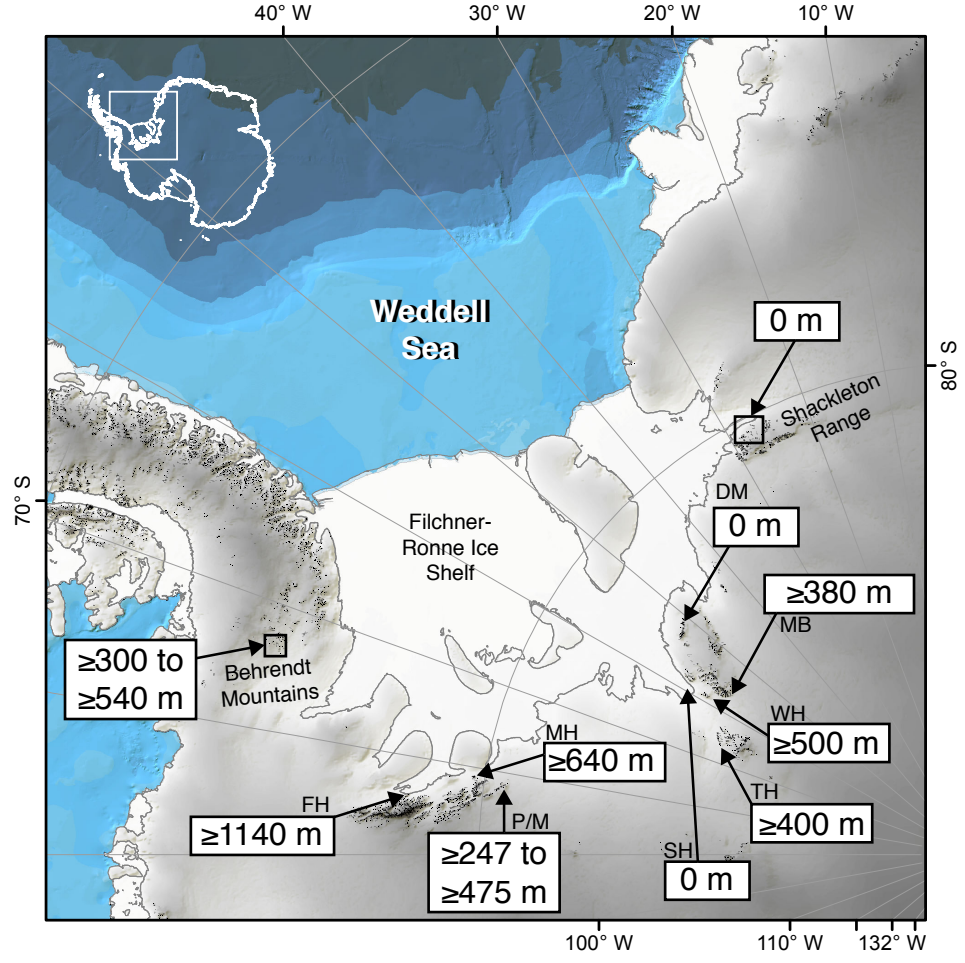

Fig. 2

The Cryosphere Discuss., https://doi.org/10.5194/tc-2019-64
Manuscript under review for journal The Cryosphere
Discussion started: 14 May 2019

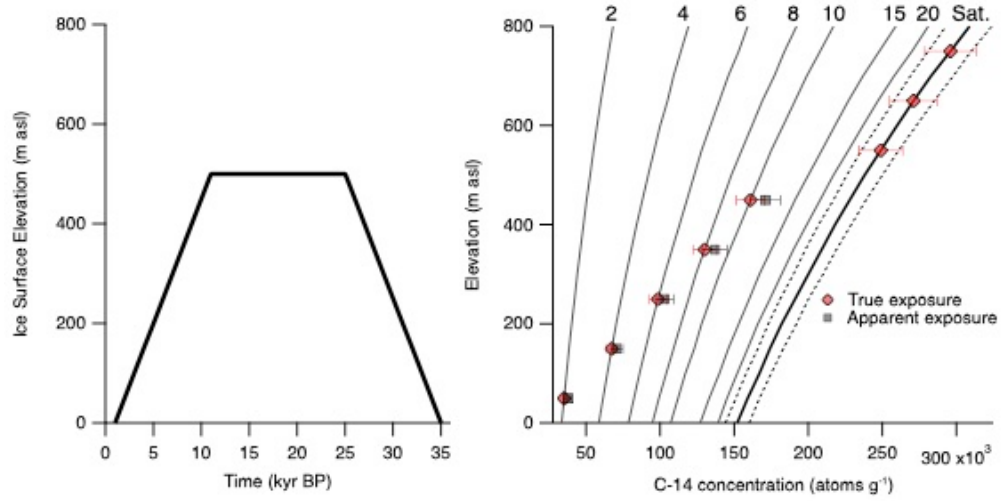

Fig. 3

The Cryosphere Discuss., https://doi.org/10.5194/tc-2019-64
Manuscript under review for journal The Cryosphere
Discussion started: 14 May 2019

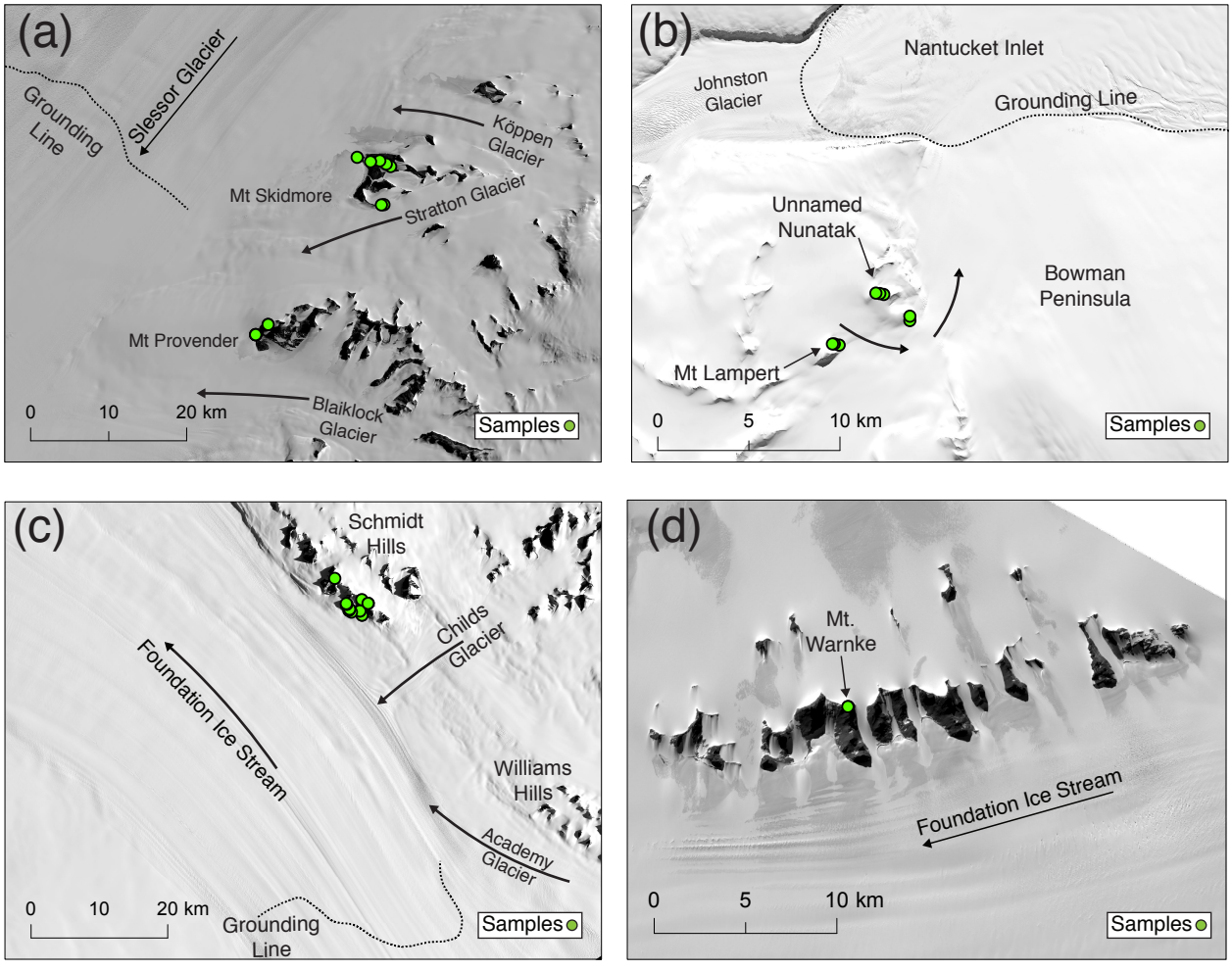

Fig. 4

The Cryosphere Discuss., https://doi.org/10.5194/tc-2019-64
Manuscript under review for journal The Cryosphere
Discussion started: 14 May 2019

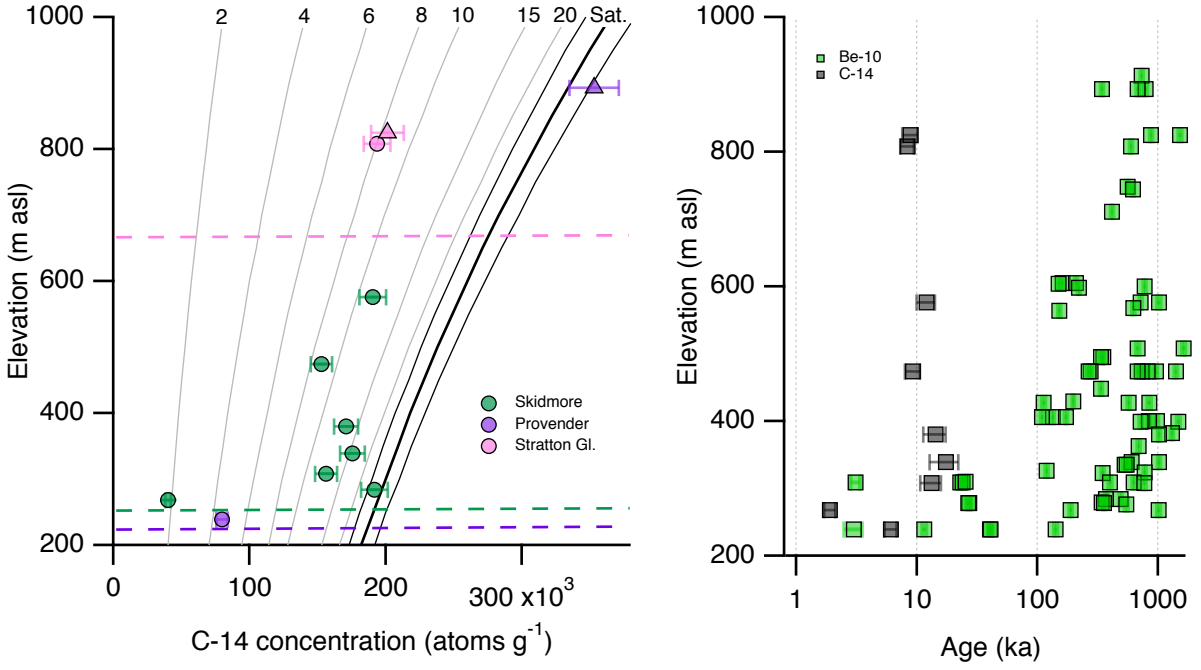

Fig. 5

5

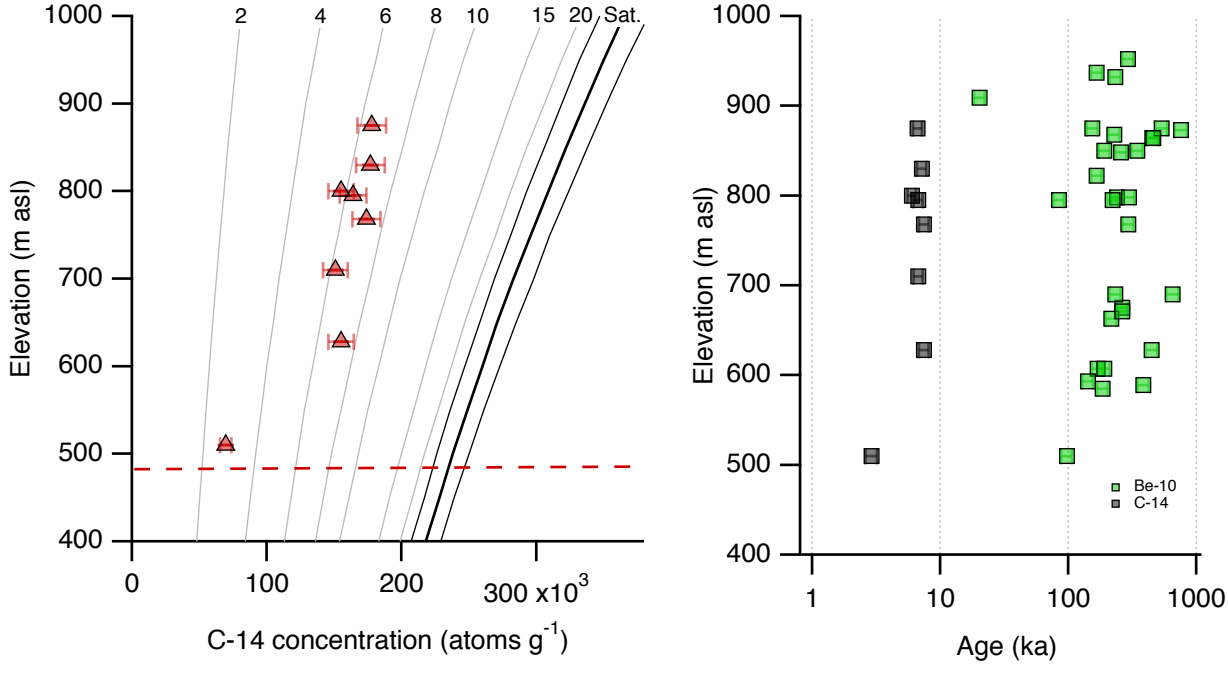

Fig. 6

The Cryosphere Discuss., https://doi.org/10.5194/tc-2019-64
Manuscript under review for journal The Cryosphere
Discussion started: 14 May 2019

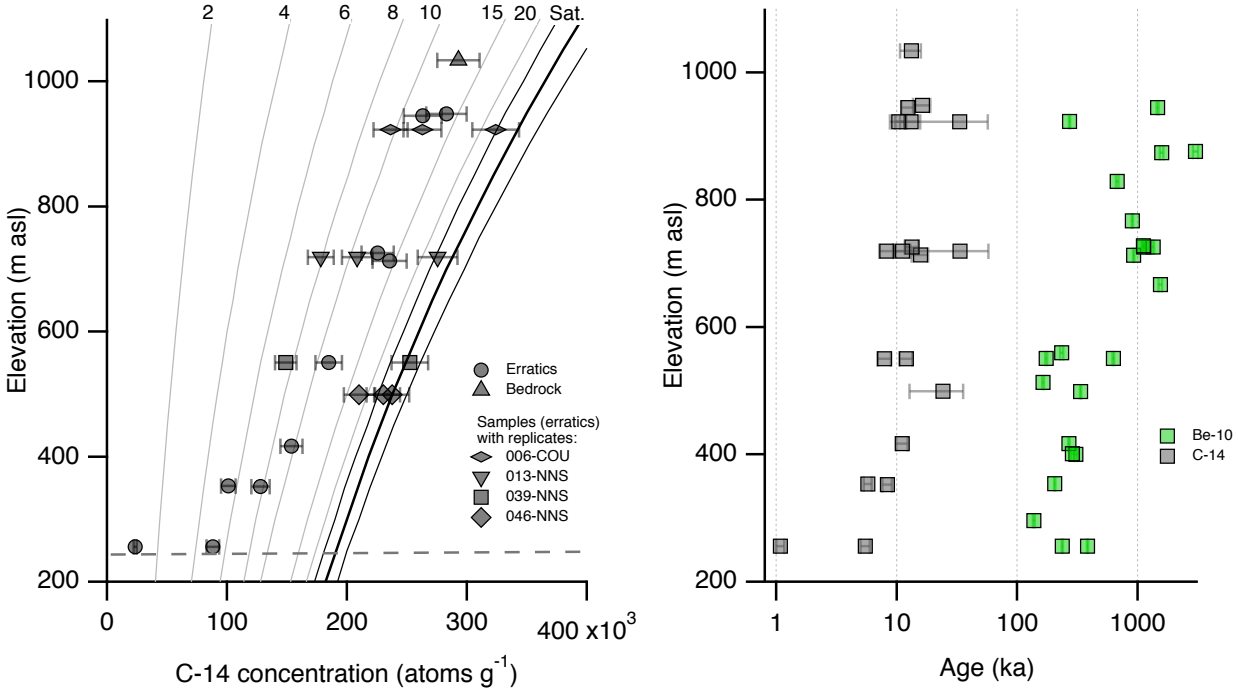

Fig. 7

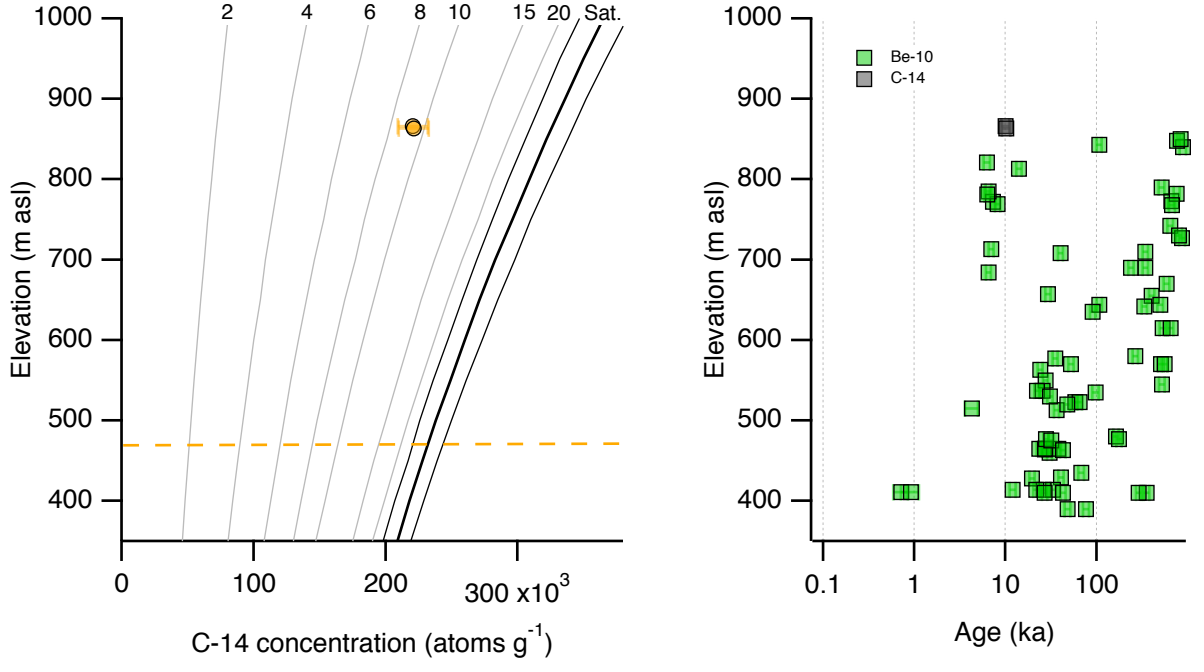

Fig. 8

The Cryosphere Discuss., https://doi.org/10.5194/tc-2019-64
Manuscript under review for journal The Cryosphere
Discussion started: 14 May 2019

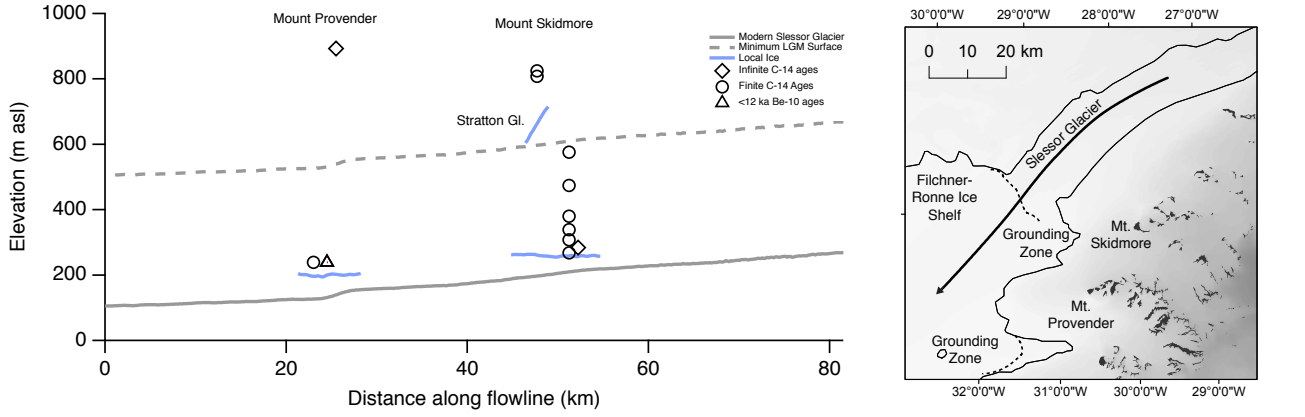

Fig. 9

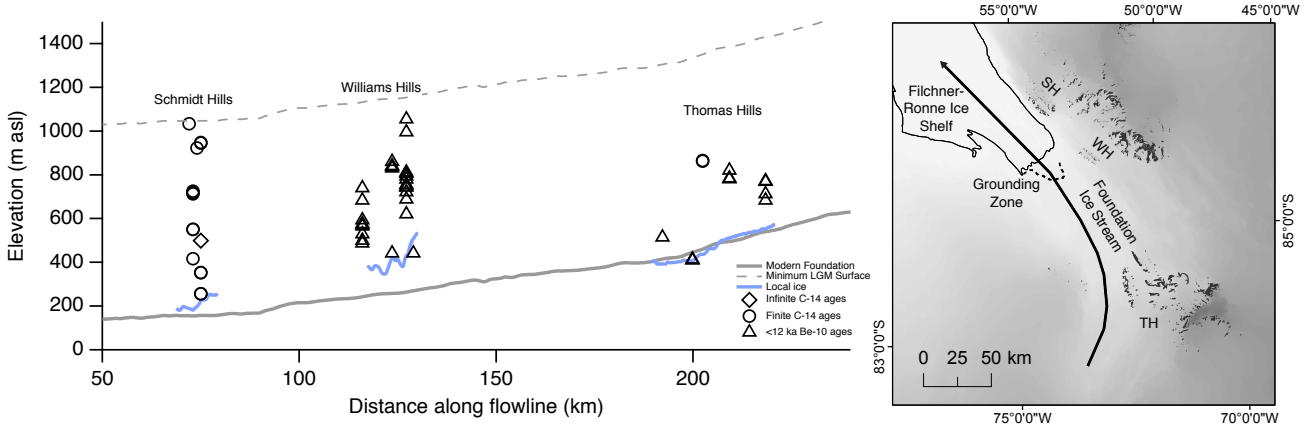

Fig. 10